Middle East Journal of Applied Sciences
Volume: 13 | Issue: 04| Oct. – Dec. | 2023

EISSN: 2706 -7947 ISSN: 2077- 4613
DOI: 10.36632/mejas/2023.13.4.54
Journal homepage: www.curresweb.com
Pages: 756-772

Biosynthesis of Zinc Nanoparticles Using Endophytic Fungi and Olive Mill Wastes and Its Activity against Some Plant Pathogenic Fungi

Ahmed I. S. Ahmed

Plant Protection Department, Desert Research Center, Cairo, Egypt

Received: 20 Sept. 2023 **Accepted:** 30 Nov. 2023 **Published:** 30 Dec. 2023

ABSTRACT

Soil-borne fungal pathogens represent a major threat to potato cultivation, particularly under arid conditions where disease management options are limited. This study aimed to explore the dual role of endophytic fungi as both biocontrol agents and biofactories for zinc nanoparticles (ZnNPs), providing an eco-friendly approach to disease suppression. Sixty symptomatic potato plants were collected from Mut and Balat, New Valley Governorate, Egypt. Six pathogenic fungi were isolated and identified, with *Fusarium oxysporum*, *F. moniliforme*, and *Rhizoctonia solani* showing the highest virulence in greenhouse assays. In parallel, twenty-two endophytic fungal isolates were obtained from healthy potato plants and screened for pathogenicity. All proved non-pathogenic were further evaluated for antagonistic activity against the pathogens. *Trichoderma sp.* and *Penicillium sp.* displayed the highest inhibition rates in dual culture assays, while *Fusarium spp.* and *Aspergillus sp.* were selected for ZnNPs biosynthesis due to their moderate antagonistic potential and superior nanoparticle production capacity. ZnNPs were synthesized using both fungal biomass and olive mill waste (OMW) and characterized via UV–Visible spectrophotometry, with absorption peaks ranging from 365 to 390 nm. *In vitro* assays revealed that endophyte-derived ZnNPs (EF-ZnNPs) had significantly higher antifungal activity than OMW-derived ZnNPs, especially at 150 ppm concentration. EF-ZnNPs inhibited radial growth and reduced dry mycelial weight of pathogens more effectively. Greenhouse trials confirmed that EF-ZnNPs reduced disease severity by up to 68% and decreased rhizosphere fungal load by over 50%, while also improving plant growth performance. These findings highlight the potential of endophytic fungi as a sustainable tool for disease control in potato cultivation, combining direct antagonism and nanotechnology-based intervention. Further studies on biosafety and environmental impact are recommended to support field-scale application.

Keywords: biological control, green synthesis, olive mill waste, rhizosphere, nanobiotechnology.

1. Introduction

Nanotechnology has rapidly become an essential component in the evolution of sustainable agriculture. By enabling the manipulation of materials at the nanoscale, this field offers promising solutions for enhancing plant growth, improving disease resistance, and minimizing the reliance on synthetic agrochemicals. Among various nanomaterials, zinc nanoparticles (ZnNPs) stand out due to their dual functional properties: they serve as an essential micronutrient and exhibit strong antimicrobial activity against a wide range of phytopathogens (Iavicoli *et al*., 2017).

Zinc plays a vital role in plant physiology, including enzyme activation, protein synthesis, and regulation of growth hormones. When applied in nanoparticle form, its bioavailability and efficacy are significantly enhanced, providing both nutritional and protective functions. However, the conventional synthesis of metal nanoparticles typically involves physical or chemical methods that require high energy input and toxic reagents, raising concerns over environmental safety and cost effectiveness (Mousa *et al*., 2022; Iravani *et al*., 2023). To address these concerns, there has been growing interest in green synthesis approaches using biological systems. Among these, endophytic fungi have proven to

Corresponding Author: Ahmed I. S. Ahmed, Plant Protection Department, Desert Research Center, Cairo, Egypt. E-mail: - ahmed_drc@yahoo.com

be effective biological agents for the biosynthesis of metal nanoparticles due to their ability to secrete extracellular enzymes and metabolites that act as natural reducers and stabilizers (Fadiji *et al*., 2022). These fungi inhabit internal plant tissues without causing disease and are known for their biocompatibility and adaptability under various environmental conditions. In parallel, the utilization of agro-industrial waste materials such as olive mill waste (OMW) has emerged as an environmentally friendly and economically viable alternative in nanoparticle synthesis. Rich in polyphenols, sugars, and organic acids, OMW offers natural reducing and capping agents that facilitate the formation and stabilization of nanoparticles (Elsayed *et al*., 2020). Its reuse not only supports sustainable nanoparticle production but also contributes to the valorisation of agricultural waste and reduction of environmental pollution. In the context of plant pathology, ZnNPs have been increasingly studied for their antifungal activity. They can disrupt the cell membranes of fungi, generate reactive oxygen species (ROS), and interfere with vital cellular processes, thereby inhibiting fungal growth and reproduction (He *et al*., 2020). This is particularly relevant for soil-borne pathogens such as *Fusarium solani*, *Rhizoctonia solani*, and *Sclerotium rolfsii*, which cause root and crown rot diseases in economically important crops like potato (*Solanum tuberosum*) (Rajani *et al*., 2022). The limitations of conventional fungicides ranging from resistance development to environmental contamination highlight the urgent need for safe and sustainable alternatives.

This study aims to compare two biological approaches for the synthesis of zinc nanoparticles one using endophytic fungi and the other using olive mill waste to evaluate their antifungal efficacy against selected root pathogens of potato.

2. Materials and Methods

2.1. Isolation and identification of pathogenic fungi from diseased potato plants

Potato plants exhibiting characteristic symptoms of root rot and damping-off (e.g., wilting, necrotic roots, and stem base discoloration) were collected from open field cultivation sites. Infected root and stem tissues were cut into small segments, surface-sterilized by sequential immersion in 70% ethanol for 30 seconds, 1% sodium hypochlorite for 3 minutes, and rinsed three times in sterile distilled water. The sterilized segments were placed on Potato Dextrose Agar (PDA; HiMedia, India) supplemented with chloramphenicol (100 µg/mL) to suppress bacterial contamination. Plates were incubated at 25 ± 2°C for 5–7 days in the dark. Emerging fungal colonies were sub-cultured on fresh PDA to obtain pure isolates. Pathogenic fungi were preliminarily identified based on colony morphology, pigmentation, and microscopic examination of spores and hyphae using lactophenol cotton blue staining. Final identification was confirmed using taxonomic keys described by Barnett and Hunter (1972) and Nelson *et al.* (1983).

2.2. Isolation and identification of endophytic fungi from healthy plant tissues

Healthy, asymptomatic plant samples (roots, stems, and leaves) were collected from wild and cultivated hosts, placed in sterile polyethylene bags, and processed within 24 h. Surface sterilization was performed by sequential washing in running water, immersion in 70% ethanol (1 min), and 1.5% sodium hypochlorite (3–5 min), followed by three rinses in sterile distilled water. Sterility was confirmed by plating the final rinse water and tissue imprints on PDA. Sterilized tissues (~0.5 cm^2) were placed on PDA supplemented with chloramphenicol (100 µg/mL) and incubated at 25 ± 2 °C in the dark for 5–7 days. Emerging colonies were sub-cultured to obtain pure isolates, maintained on PDA slants at 4 °C, and cryopreserved in 20% glycerol at –20 °C. Preliminary identification was based on macroscopic and microscopic features (colony morphology, pigmentation, conidial structures, septation, branching), using lactophenol cotton blue staining. Taxonomic assignment to genus level followed the keys of Barnett and Hunter (1972) and Domsch *et al*. (2007), with reference to published descriptions. Only non-pathogenic isolates with consistent morphology were selected for subsequent nanoparticle biosynthesis and antagonistic assays.

2.3. Pathogenicity testing of endophytic fungi

Pathogenicity of selected endophytic isolates was evaluated under greenhouse conditions to ensure biosafety prior to ZnNP biosynthesis. Isolates were grown on PDA at 25 ± 2 °C for 7 days, and spore suspensions (1×10^6 spores/mL) were prepared in sterile distilled water with 0.01% Tween 80,

following Schulz and Boyle (2005) and Strobel and Daisy (2003). Surface-sterilized, certified disease-free potato tubers (cv. Spunta) were planted in autoclaved loamy soil. After seedling emergence, 20 mL of spore suspension was applied at the plant base; controls received sterile water with Tween 80 only. Each treatment included five replicates. Plants were maintained at 25–30 °C and 60–70% RH for 21 days, with symptom assessment based on McGovern (2015). Isolates causing no visible disease symptoms or growth reduction compared to controls were classified as non-pathogenic and retained for subsequent nanoparticle biosynthesis experiments.

2.4. *In vitro* assay: mycelial growth and colonization potential

Fungal isolates were cultured on PDA supplemented with 5% (v/v) sterile-filtered potato root extract to simulate host nutrient conditions and promote aggressiveness (Ondřej et al., 2008). A 5 mm mycelial disc from the actively growing edge of a 7-day-old colony was centrally placed on each plate. Cultures were incubated at 25 ± 2 °C for 7 days, with radial growth measured daily along two perpendicular axes to calculate mean growth rate (mm/day). Colony margin characteristics (regular, wavy, or irregular) and sporulation density were recorded as indicators of pathogenic vigor (Leslie and Summerell, 2006). Each isolate was assessed in triplicate, and comparative analysis was used to rank isolates by aggressiveness, with the most rapidly growing and profusely sporulating isolates selected for further in vivo pathogenicity evaluation.

2.5. *In vivo* assay: disease development under greenhouse conditions

Confirm pathogenicity under semi-natural conditions. Inoculum was produced by culturing the selected fungi on autoclaved wheat grains (1:1 w/v soaked grains to water) in 500 mL Erlenmeyer flasks and incubating at 25 °C for 10–12 days with intermittent shaking to ensure uniform colonization (Singh and Kumar, 2011). Colonized grains were mixed with autoclaved loamy soil at a ratio of 1:10 (w/w) to prepare infested soil. Sterile plastic pots (30 cm diameter) were filled with the infested soil, and surface-disinfected seed tubers of *Solanum tuberosum* cv. Spunta (treated with 1% sodium hypochlorite) were planted at a depth of 5–7 cm. Each treatment comprised five replicate pots, while control plants were grown in sterilized, non-infested soil. Plants were maintained under greenhouse conditions (25–30 °C, 60–70% relative humidity, 12 h light/dark cycle) and irrigated as needed. Disease symptoms were monitored for 30 days post-planting and assessed using a modified 0–5 scale (0 = healthy; 5 = complete collapse or extensive root rot) as per McGovern (2015). The Disease Severity Index (DSI) was calculated according to:

$$\text{DSI } \% = \frac{\sum(n \times r)}{N \times R} \times 100$$

where n is the number of plants in each rating category, r is the corresponding rating value, N is the total number of assessed plants, and R is the maximum rating value (5). Post-assessment, root systems were examined for internal browning, cortical decay, and vascular discoloration to confirm virulence and validate isolate selection for subsequent antifungal evaluation.

2.6. Biosynthesis of zinc nanoparticles using non-pathogenic endophytic fungi

Non-pathogenic endophytic fungal isolates, previously confirmed via greenhouse pathogenicity tests, were employed for green synthesis of zinc nanoparticles (ZnNPs), utilizing extracellular fungal metabolites as reducing and capping agents (Iravani, 2011). Fungi were cultured on Potato Dextrose Agar (PDA) at 25 ± 2 °C for 7 days, and 5 mm mycelial discs from actively growing margins were transferred to 250 mL Erlenmeyer flasks containing 100 mL sterile Czapek Dox broth. Cultures were incubated at 28 ± 2 °C under static conditions for 5 days (Hasansab *et al*., 2022). Biomass was separated by filtration through Whatman No. 1 paper, and the cell-free culture filtrate (CFCF) was used as the reaction medium. Zinc nitrate hexahydrate [$Zn(NO_3)_2 \cdot 6H_2O$] was added to the CFCF to a final concentration of 2 mM, and the mixture was incubated in the dark at ambient temperature for 72 h to prevent photoreduction (Raliya *et al*., 2013). A progressive color change from pale yellow to brownish-yellow indicated nanoparticle formation, absent in controls containing either zinc nitrate or CFCF alone. The ZnNP suspension was centrifuged at 10,000 rpm for 15 min to remove residual biomass and stored

at 4 °C in amber vials. Synthesis was verified by UV–Vis spectrophotometry, and the resulting ZnNPs were directly applied in subsequent *in vitro* and *in vivo* antifungal assays.

2.7. Green synthesis of zinc nanoparticles using olive mill waste (omw)

Olive mill waste (OMW) was sourced from a local olive oil processing unit, oven-dried at 60 °C for 48h, and finely milled. A 20 g/L aqueous suspension was prepared using distilled water and sterilized by autoclaving at 121 °C for 15 min. Following cooling, zinc nitrate hexahydrate [$Zn(NO_3)_2 \cdot 6H_2O$] was incorporated into the sterile extract to achieve a final concentration of 2 mM. The mixture was maintained under static, dark conditions at 28 ± 2 °C for 5–7 days, during which color change served as a visual indicator of nanoparticle formation. The reaction product was subsequently filtered through Whatman No. 1 paper, and the ZnNP-containing filtrate was stored at 4 °C for subsequent applications (Russo *et al*., 2022).

2.8. Screening of endophytic fungi for antagonistic activity

Non-pathogenic endophytic fungal isolates were screened for antagonism against target phytopathogens using a dual culture assay on PDA medium. In each 90 mm Petri plate, a 5 mm plug of the pathogen (7-day-old culture) was placed 10 mm from the plate edge, with an opposing 5 mm plug of the endophyte positioned equidistant on the opposite side. Controls comprised pathogen inoculation without the antagonist.

Plates were incubated at 25 ± 2 °C for 7 days in darkness, with three replicates per treatment. Antagonistic efficacy was quantified by calculating the percentage inhibition of radial growth (PIRG) according to Dennis and Webster (1971):

$$PIRG\% = \frac{R1 - R2}{R1} \times 100$$

where R1R_1R1 is the radial growth of the pathogen in control plates, and R2R_2R2 is its growth toward the antagonist. Interaction types, including overgrowth, contact inhibition, and inhibition zones, were classified following Bell *et al*. (1982).

2.9. *In vitro* evaluation of biosynthesized ZnNPs at different concentrations

The antifungal potential of biosynthesized zinc nanoparticles (ZnNPs) from endophytic fungi and olive mill waste (OMW) was tested at 25, 50, 75, 100, and 150 ppm using standardized in vitro assays. Both ZnNP types were evaluated under identical conditions to facilitate direct comparison. Pathogen cultures were exposed to each treatment, and growth inhibition was recorded to determine concentration-dependent efficacy.

2.10. Radial growth inhibition assay

PDA medium was amended with the respective ZnNP concentrations before pouring into sterile 90 mm Petri dishes (20 mL per plate). A 5 mm mycelial disc from the edge of a 7-day-old pathogenic fungal culture was centrally placed on each plate. Plates were incubated at 25 ± 2°C for 7 days. Fungal colony diameter was measured along two perpendicular lines, and average radial growth was recorded. The percentage inhibition of mycelial growth was calculated relative to the control (ZnNP-free PDA) using the formula by Vincent (1947):

$$Inhibition\ (\%) = \frac{C - T}{C}\%$$

Where, C = radial growth in the control, T = radial growth in the treatment and each treatment was performed in triplicate.

2.11. Dry mycelial weight assay and spore morphology observation

Mycelial biomass production was assessed in Potato Dextrose Broth (PDB) amended with the specified concentrations of ZnNPs. Aliquots of 100 mL PDB were dispensed into 250 mL Erlenmeyer flasks and inoculated with a 5 mm agar plug from the actively growing margin of the test pathogen. Cultures were incubated statically at 25 °C for 7 days. Following incubation, the mycelial mats were collected by filtration through pre-weighed Whatman No. 1 filter papers, rinsed thoroughly with sterile

distilled water to remove residual medium, and dried at 60 °C until constant weight was achieved. Biomass was expressed as mean dry weight (mg) and compared statistically with the untreated control (Techaoei *et al*. 2020).

Spore suspensions (1×10^6 spores/mL) were treated with 100 ppm ZnNPs and incubated for 24 hours at room temperature. A drop of the treated suspension was examined under a compound microscope (400× magnification) to detect any morphological alterations or deformities in spore structure (Mosquera-Sánchez *et al*., 2020). Control slides (untreated spores) were used for comparison.

2.12. Greenhouse evaluation of the most effective ZnNPs concentrations

Greenhouse trials were conducted to validate the efficacy of the two most potent concentrations of each ZnNP formulation (fungal-derived and olive mill waste-derived), as determined by *in vitro* antifungal screening, in suppressing disease symptoms and enhancing potato growth under semi-controlled conditions. Loamy soil was double-autoclaved at 121°C for 60 min on two consecutive days and subsequently infested with wheat-grain inoculum as growth media of the target pathogen, prepared by incubating sterilized grains with fungal cultures for 10 days at 25 °C, at a ratio of 1:10 (w/w) (McGovern, 2015). Sterilized plastic pots (30 cm diameter) were filled with 5 kg of infested soil, while non-infested sterile soil served as the healthy control. Certified disease-free potato tubers (cv. Spunta) were surface disinfected with 1% sodium hypochlorite for 3 min, rinsed thoroughly in sterile distilled water, and planted (one tuber per pot). Immediately after planting, ZnNP suspensions at the selected concentrations (100 and 150 ppm) were applied as soil drenches at 100 mL per pot (El-Shafei *et al*., 2020). The experimental layout followed a completely randomized design (CRD) with five replicates per treatment, including negative (healthy soil, no pathogen or ZnNPs), positive (infested soil, no ZnNPs), and ZnNP-only (healthy soil with ZnNPs) controls. Plants were maintained in a greenhouse at 25–30 °C with regular irrigation. After 30 days, disease severity was assessed on a 0–5 scale based on root discoloration, lesion development, and wilting (Bell *et al*., 1982), and both disease incidence (%) and disease severity index (DSI) were calculated using the formula of McKinney (1923). Plant growth responses, including shoot height, root length, and fresh and dry biomass, were also recorded for each treatment.

2.13. Evaluation of total fungal count in soil (rhizosphere) under greenhouse conditions

To evaluate the impact of biosynthesized zinc nanoparticles (ZnNPs) on rhizospheric fungal populations, soil samples were collected from the root zone of each pot at the end of the greenhouse trial (30 days post-planting). Approximately 10 g of soil was obtained after removing coarse debris and root fragments, transferred to sterile polyethylene bags, and processed immediately or stored at 4 °C for no longer than 24 h (Domsch *et al*., 2007). One gram of each sample was suspended in 9 mL of sterile distilled water and serially diluted to 10^{-4}. From each dilution, 1 mL aliquots were spread on Potato Dextrose Agar (PDA) plates supplemented with chloramphenicol (100 mg/L) to inhibit bacterial growth (Atlas and Parks, 1997). Plates were incubated at 25 ± 2 °C for 5–7 days, after which fungal colonies were counted, and total fungal load was expressed as colony-forming units per gram of dry soil (CFU g^{-1}) using the formula:

$$CFU/g\ soil = \frac{\text{Number of colonies} \times \text{dilution factor}}{\text{volume plated (ml)}}$$

2.14. Statistical analysis

All experimental datasets covering growth inhibition, mycelial biomass, disease severity, plant performance, and rhizospheric fungal populations were analyzed using one-way ANOVA, with treatment means separated by Duncan's Multiple Range Test at $P \leq 0.05$. Analyses were conducted in IBM SPSS Statistics v25.0 (IBM Corp., Armonk, NY, USA), and results are expressed as mean ± SE, with figures generated in Microsoft Excel 2019.

3. Results and Discussion

3.1. Isolation and identification of fungal pathogens

During September to January 2021/2022 winter season, sixty diseased potato samples were collected from Mut and Balat, key potato-producing areas in the New Valley Governorate, Egypt. These regions, characterized by sandy-loamy soils and an arid climate, provide favourable conditions for soil-borne diseases. Fungal isolation from infected root and stem tissues consistently yielded six phytopathogenic species: *F. oxysporum, F. moniliforme, F. solani, Rhizoctonia solani, Macrophomina phaseolina,* and *Pythium ultimum* (Table 1). *F. oxysporum* was the most prevalent, the frequent occurrence of *F. moniliforme, F. solani* reflects their association with dry rot and vascular wilt, particularly under fluctuating soil moisture conditions. The relatively lower incidence of *R. solani* (10%) is consistent with its behavior as an opportunistic pathogen linked to damping-off and stem canker under poorly drained or suboptimal field conditions. Overall, the predominance of *F. oxysporum* and *F. moniliforme* indicates their ecological adaptability and persistence under New Valley conditions, reinforcing the importance of locally adapted, integrated disease management approaches, these findings are largely consistent with previous studies that reported the significant involvement of these pathogens in potato wilt, root rot, and dry rot diseases under Egyptian conditions (Saber *et al*., 2013; Azil *et al*., 2021; Attia *et al*., 2019).

Table 1: Frequency of pathogenic fungal species isolated from infected potato plants in Mut and Balat (New Valley Governorate)

Fungal species	Frequency of isolation (%)	Relative rank
Fusarium oxysporum	36.7%	Most frequent
Fusarium moniliforme	20.0%	Moderately frequent
Fusarium solani	13.3%	Moderately frequent
Rhizoctonia solani	10.0%	Occasional
Macrophomina phaseolina	12.0%	Occasional
Pythium ultimum	08.0%	Least frequent

Note: Percentages based on total isolates from 60 composite samples; identification was confirmed based on morphological features on PDA and microscopy.

3.2. Isolation and identification of endophytic fungi from healthy potato plants

During the winter season (September–January 2021/2022), thirty asymptomatic potato plants were collected from the same fields in Mut and Balat, New Valley Governorate, Egypt, previously surveyed for pathogen isolation. This agriculturally important region, characterized by a semi-arid climate, offers conditions conducive to distinctive endophytic assemblages. Root, stem, and leaf tissues were subjected to standard surface sterilization (70% ethanol for 1 min, followed by 1.5% sodium hypochlorite for 3 min, and triple rinsing with sterile distilled water). Sterilization efficiency was confirmed via PDA imprint tests, which yielded no microbial growth.

From the internal tissues, twenty-two fungal isolates representing six genera were recovered. The most abundant taxa were *Penicillium* (27.3%), *Trichoderma* (22.7%), and *Aspergillus* (18.2%), with the remainder comprising *Alternaria*, *Cladosporium*, and *Fusarium* spp. (Table 2). The predominance of *Penicillium* and *Trichoderma* is consistent with earlier reports of their frequent occurrence as dominant endophytes in solanaceous hosts grown under arid and semi-arid conditions, reflecting their ecological resilience, tissue-colonizing capacity, and documented biocontrol potential (Zachary *et al*., 2022; El Debaiky and El Sayed, 2023).

The detection of *Fusarium* spp. among endophytes, despite the pathogenic reputation of many of its members, highlights the functional plasticity of certain fungal taxa, which may adopt endophytic lifestyles under specific environmental or host developmental contexts (Strobel and Daisy, 2003). The isolation of *Alternaria*, *Cladosporium*, and *Aspergillus* further supports their reported roles in plant defence modulation and secondary metabolite production as components of the endophytic microbiome.

Overall, these results demonstrate the taxonomic diversity of fungal endophytes in symptom-free potato tissues cultivated in semi-arid systems and underline their potential value for biotechnological applications, including nanoparticle biosynthesis, warranting further functional characterization.

Table 2: Frequency and distribution of endophytic fungi isolated from healthy potato tissues (n = 25 plants)

Genus	No. of isolates	Frequency (%)	Tissue source
Penicillium	6	27.3	Roots, basal stems
Trichoderma	5	22.7	Roots, stems
Aspergillus	4	18.2	Roots
Cladosporium	4	18.2	Leaves, stems
Alternaria	2	9.1	Leaves
***Fusarium* spp.**	1	4.5	Roots
Total	22	100	

3.3. Pathogenicity assessment of endophytic fungal isolates

To confirm the biosafety of the 22 endophytic fungal isolates prior to their application as biological agents, a pathogenicity assay was conducted under greenhouse conditions. This step was essential to ensure that none of the isolates could induce disease symptoms before their subsequent use in antagonism assays or zinc nanoparticle (ZnNP) biosynthesis. The study compared three antifungal approaches: (1) direct application of endophytes, (2) ZnNPs produced by endophytes, and (3) ZnNPs synthesized from olive mill waste. Healthy potato tubers (*Solanum tuberosum* cv. Spunta) were planted in sterile loamy soil within plastic pots. Each isolate was applied as a 10 mL soil drench containing a spore suspension (1×10^6 spores mL^{-1}) around the root zone, while control pots received sterile distilled water. Plants were maintained in a greenhouse at 24–28 °C under optimal moisture and monitored for 21 days. Disease symptoms including stem base necrosis, wilting, stunting, or root lesions were evaluated using a 0–5 severity scale (Burlakoti *et al*., 2020). None of the inoculated plants developed visible symptoms or showed growth deviations from the control, confirming the non-pathogenic nature of all isolates (Table 3).

Table 3: Pathogenicity assessment of endophytic fungal isolates on potato plants under greenhouse conditions (21 days post-inoculation)

Endophytic isolate	Disease Severity Score (0–5)	Visual symptoms	Remarks
***Trichoderma* sp.**	0.0 ± 0.00	None	Non-pathogenic
***Penicillium* sp.**	0.0 ± 0.00	None	Non-pathogenic
***Aspergillus* sp.**	0.2 ± 0.05	Slight yellowing (rare)	Non-significant vs. control
***Cladosporium* sp.**	0.0 ± 0.00	None	Non-pathogenic
***Alternaria* sp.**	0.3 ± 0.10	Mild leaf curling	Within safe threshold
***Fusarium* spp. (endophyte)**	0.2 ± 0.06	Slight root browning	Non-significant vs. control
Control (water)	0.0 ± 0.00	None	Healthy control

Disease severity scored using a 0–5 scale adapted from Burlakoti *et al.,* (2020).

These observations are consistent with previous reports describing *Penicillium*, *Trichoderma*, and *Cladosporium* species as non-pathogenic endophytes with potential plant growth-promoting effects under stress conditions (Zachary *et al*., 2022; Strobel and Daisy, 2003). All isolates were therefore retained for further testing. Strains exhibiting strong antagonism toward pathogenic fungi were prioritised for direct biocontrol applications, while those with minimal antagonistic activity were employed for ZnNP production, enabling evaluation of their indirect antifungal effects. This dual-use strategy supports the integration of endophytes as both biological control agents and nanoparticle biofactories within sustainable disease management frameworks.

3.4. *In vitro* antagonistic activity of endophytic fungi against pathogenic isolates

The antagonistic potential of six endophytic fungal genera was assessed using a dual culture assay against five major pathogenic fungi isolated from diseased potato plants. The inhibition percentages of radial growth varied significantly among isolates and target pathogens as illustrated in (Table 4).

Trichoderma sp. consistently exhibited the highest antifungal activity across all tested pathogens, with inhibition values ranging from 57.7% against *Pythium ultimum* to 71.9% against *Fusarium oxysporum*. These results reinforce the well-established mycoparasitic and enzyme-producing capabilities of *Trichoderma*, which enable it to degrade pathogen cell walls and outcompete pathogens *in vitro* (Harman *et al*., 2004; Mukherjee *et al.,* 2020). *Penicillium* sp. showed similarly strong antagonistic performance, with inhibition levels between 52.5% and 66.9%. Its efficacy is attributed to the secretion of antifungal metabolites such as *penicillinic* acid derivatives and its rapid colonization behaviour. *Aspergillus* spp. and *Cladosporium* spp. exhibited moderate inhibitory effects. *Aspergillus* reached up to 57.5% inhibition against *F. oxysporum*, but its performance declined across other pathogens. While *Aspergillus* is not traditionally considered a frontline biocontrol agent, some strains produce secondary metabolites with antifungal properties (Zachary *et al*., 2022). *Alternaria* sp. showed limited antagonism with inhibition values not exceeding 48.6%, whereas endophytic *Fusarium* spp. exhibited the weakest inhibition (24.3–33.6%). These results are expected, as most *Fusarium* species act as facultative pathogens and lack competitive antifungal mechanisms (Abo-Elyousr *et al*., 2012). The findings demonstrate clear isolate-specific antagonistic effects, suggesting that *Trichoderma* sp. and *Penicillium* sp. possess the most promising attributes for biocontrol applications or as biofactories for ZnNPs. The limited antifungal potential of endophytic *Fusarium* isolates justifies their use in nanoparticle biosynthesis, rather than direct biocontrol.

Table 4: *In vitro* antagonistic activity (%) of endophytic fungal isolates against major potato pathogens in dual culture assay.

Endophytic Isolate	*F. oxysporum*	*F. solani*	*R. solani*	*M. phaseolina*	*P. ultimum*
***Trichoderma* sp.**	71.9 ± 1.1^{a}	68.8 ± 1.4^{a}	64.2 ± 1.2^{b}	60.1 ± 1.5^{c}	57.7 ± 1.3^{d}
***Penicillium* sp.**	66.9 ± 1.2^{a}	61.8 ± 1.4^{b}	59.8 ± 1.7^{bc}	55.6 ± 1.8^{c}	52.5 ± 1.7^{d}
***Aspergillus* sp.**	57.5 ± 1.2^{a}	52.8 ± 1.4^{b}	48.7 ± 1.7^{c}	44.6 ± 1.9^{d}	41.9 ± 1.7^{e}
***Cladosporium* sp.**	56.1 ± 1.3^{a}	51.9 ± 1.1^{ab}	47.3 ± 1.2^{b}	43.8 ± 1.1^{c}	40.5 ± 1.3^{c}
***Alternaria* sp.**	48.6 ± 1.5^{a}	44.4 ± 1.3^{b}	40.9 ± 1.5^{c}	38.2 ± 1.7^{c}	35.1 ± 1.6^{c}
***Fusarium* spp.**	33.6 ± 1.4^{a}	30.9 ± 1.2^{a}	27.4 ± 1.5^{b}	26.1 ± 1.4^{b}	24.3 ± 1.2^{b}

3.5. Evaluation of pathogenicity of fungal isolates under greenhouse conditions

To determine the aggressiveness of the most frequently isolated soil-borne pathogens from diseased potato plants, greenhouse trials were conducted using sterile soil infested with fungal inocula. The aim was to confirm the in vitro findings under more realistic conditions and identify the most virulent species to be used as target pathogens in further antifungal testing.

Over a 30-day observation period, infected plants exhibited varying degrees of disease symptoms, including root discoloration, stem necrosis, wilting, and in severe cases, complete collapse. The calculated Disease Severity Index (DSI%) revealed significant differences among the fungal

species (Fig. 1). The highest DSI was recorded for *Fusarium oxysporum* (80.5% ± 1.9), indicating its strong aggressiveness and rapid colonization potential. This aligns with findings from Gherbawy *et al.* (2020) and El-Mohamedy and Abo-Elyousr (2013), where *F. oxysporum* consistently emerged as one of the most destructive soil-borne pathogens in potato fields due to its vascular invasion and systemic effects.

Fusarium moniliforme also demonstrated high virulence (73.3% ± 2.3), followed by *Rhizoctonia solani* (65.1% ± 2.5), which is known to cause crown rot and seedling damping-off, particularly under moderate soil moisture levels. These findings confirm pathogenic relevance of *R. solani* in arid and semi-arid potato zones, as reported by Aydi-Ben-Abdallah *et al*. (2020)..

Moderate disease severity was observed with *Fusarium solani* (59.4% ± 2.0), which can infect both basal stems and roots but typically produces less vascular damage than *F. oxysporum. Macrophomina phaseolina* and *Pythium ultimum* induced significantly lower DSI values (51.3% ± 1.8 and 47.6% ± 1.6, respectively), likely reflecting their preference for stress-induced or waterlogged conditions, which were not predominant during the trial period. As expected, no symptoms were observed in the non-infested control group (0.0% DSI), confirming the effectiveness of soil sterilization and the pathogenic nature of the tested fungi. These results guided the selection of the most aggressive pathogens for subsequent antifungal bioassays, particularly *F. oxysporum, F. moniliforme,* and *R. solani*, as they presented the highest disease potential under greenhouse conditions.

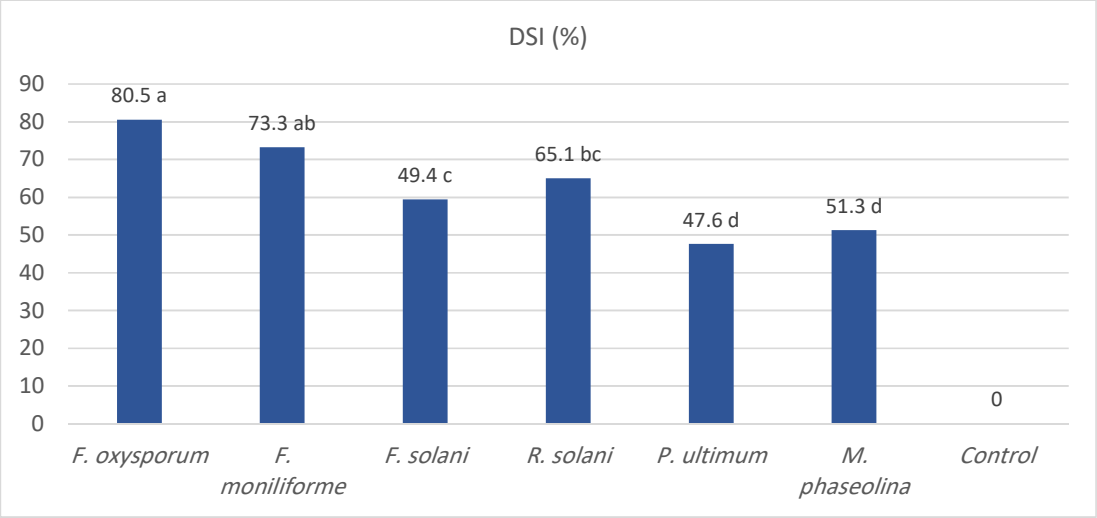

Fig. 1: Disease Severity Index (DSI%) of potato plants inoculated with pathogenic fungi under greenhouse conditions

3.6. Biosynthesis of ZnNPs using endophytic fungi

To evaluate the potential of endophytic fungi as sustainable biocatalysts for zinc nanoparticle (ZnNP) synthesis, five non-pathogenic isolates were selected based on both high and low antagonistic capacities. These included representatives from Fusarium, Aspergillus, and Alternaria genera, enabling comparison of biosynthetic efficiency across taxonomic and functional groups.

Nanoparticle synthesis was achieved by incubating cell-free fungal filtrates with zinc nitrate under static, ambient conditions. The progression of the reaction was visually indicated by a shift in color from pale yellow to varying shades of brown, attributable to surface plasmon resonance (SPR) phenomena associated with ZnNP formation (Iravani, 2011; Raliya *et al*., 2013). UV–Visible spectrophotometric analysis confirmed nanoparticle production, with absorption maxima recorded between 365 and 390 nm. Isolates of Fusarium produced peaks at 370–375 nm, Aspergillus at 365–368 nm, and Alternaria which exhibited the lowest biosynthetic capacity at approximately 387 nm, the latter indicative of broader size distribution and reduced uniformity (Table 5; Fig. 2).

Reaction kinetics varied among the isolates, with Aspergillus completing nanoparticle formation within 48–60 h, whereas Fusarium and Alternaria required up to 72 h. These interspecific differences are consistent with earlier findings linking fungal metabolic activity, enzymatic composition, and reducing potential to nanoparticle yield and quality (Narayanan and Sakthivel, 2010). The superior performance of Aspergillus suggests its suitability for rapid and efficient biotransformation processes in nanobiotechnological applications.

Collectively, the observed variability in biosynthesis efficiency supports the targeted selection of endophytic fungi for specific applications, whether in direct biocontrol or as nanoparticle biofactories, aligning with prior studies that emphasise genus-level differences in nanomaterial production potential (Jain *et al*., 2022).

Table 5: Biosynthesis parameters of ZnNPs from selected endophytic isolates

Isolate Code*	Genus	Color Change	Reaction Time (h)	UV-Vis Absorbance Peak (nm)
END-01	*Fusarium* spp.	Pale yellow → Brown	72	371
END-03	*Alternaria* sp.	Pale yellow → Yellow-brown	72	383
END-07	*Aspergillus* sp.	Pale yellow → Brown	48	364
END-12	*Fusarium* spp.	Pale yellow → Brown	72	375
END-15	*Aspergillus* sp.	Pale yellow → Light brown	60	368

* END; Endophytic Non-pathogenic Fungi.

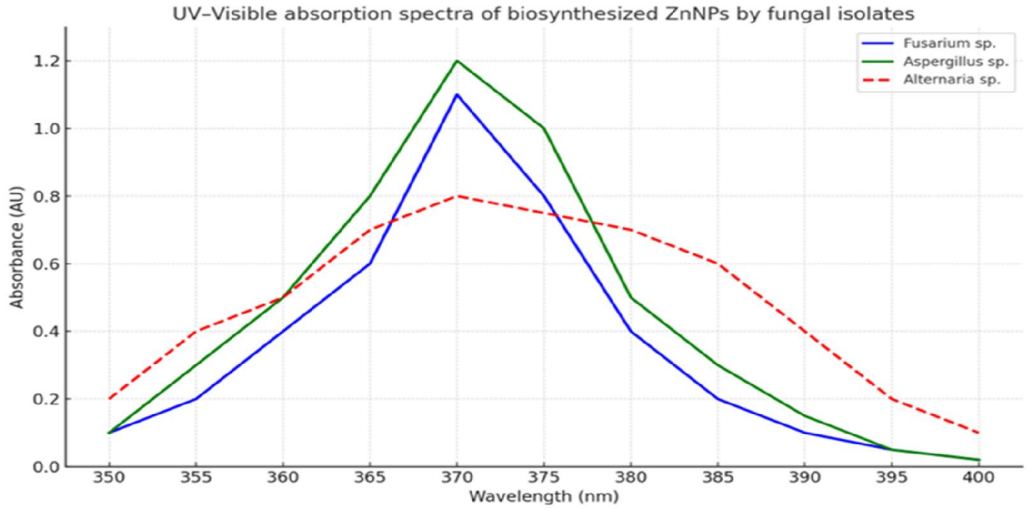

Fig. 2: UV-Visible absorption spectra confirming the biosynthesis of zinc nanoparticles (ZnNPs) by endophytic fungal isolates (*Fusarium* spp., *Aspergillus* sp., and *Alternaria* sp.) using a double-beam spectrophotometer. The illustrated absorption curves are representative diagrams based on actual UV - Vis spectrophotometric readings obtained using a double-beam system during the biosynthesis of ZnNPs.

3.7. Green synthesis of zinc nanoparticles using olive mill waste (OMW)

Olive mill waste (OMW), a lignocellulosic agro-industrial byproduct, was successfully employed as a reducing and stabilizing agent in the green synthesis of zinc nanoparticles (ZnNPs). Upon combining the sterilized OMW extract with aqueous zinc nitrate solution and incubating under static conditions, a noticeable change in the solution's color from light yellow to deep brownish-yellow was observed after 72 hours, indicating the formation of nanoparticles. The biosynthesis was further verified

using a UV–Visible spectrophotometer. The absorption spectrum revealed a broad yet distinct peak centered around 230 - 250 nm, confirming the reduction of zinc ions into nanoscale particles. Compared to the nanoparticles synthesized using fungal filtrates, the OMW-derived ZnNPs exhibited broader and less intense peaks, implying a wider particle size distribution and potentially lower stability (Figure 3). These differences may be attributed to the complex and heterogeneous nature of organic compounds in OMW, including phenolics, polysaccharides, and fatty residues, which influence the reduction kinetics and capping efficiency. Despite these variations, the OMW-derived ZnNPs were successfully collected and stored without visible aggregation, suggesting acceptable colloidal stability for short-term applications. Their subsequent evaluation in antifungal assays revealed moderate efficacy, which may relate to both particle morphology and residual organic compounds adsorbed on the surface. These findings are consistent with prior reports that emphasized the potential of agro-waste materials for nanoparticle production (Alkhalaf *et al*., 2020; De Matteis *et al.,* 2021), highlighting their value in sustainable nanotechnology and waste valorisation. Moreover, employing OMW for ZnNP synthesis not only reduces production costs but also addresses environmental concerns associated with the disposal of olive processing residues in Mediterranean regions.

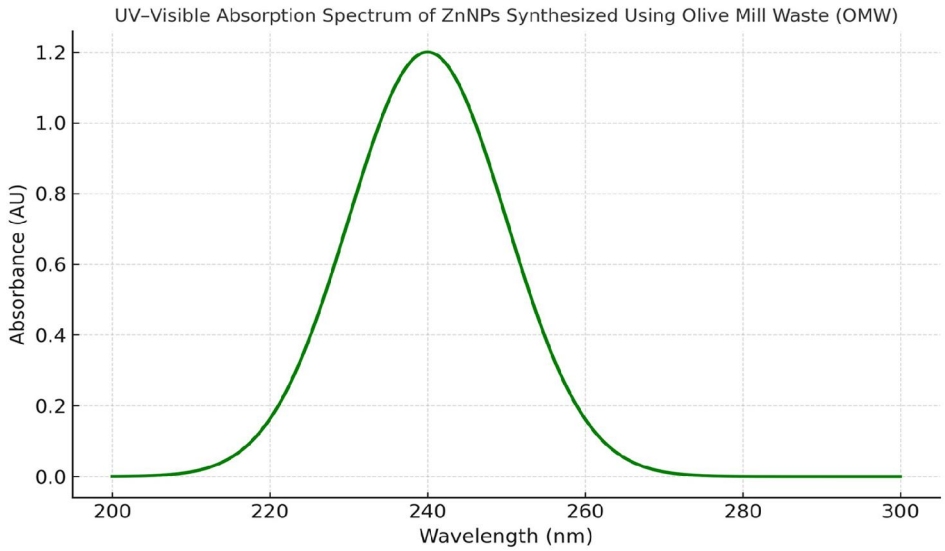

Fig. 3: UV-Visible absorption spectrum confirming the green synthesis of zinc nanoparticles (ZnNPs) using olive mill waste (OMW), as recorded with a double spectrophotometer. The illustrated absorption curve is a representative diagram derived from actual UV-Vis spectrophotometric readings, showing a characteristic peak around 240nm, which indicates the successful formation of ZnNPs through this eco-friendly approach.

3.8. *In vitro* evaluation of biosynthesized ZnNPs at different concentrations

To assess the antifungal efficacy of biosynthesized zinc nanoparticles (ZnNPs), radial growth inhibition assays were conducted against the three most virulent pathogens previously identified: *Fusarium oxysporum*, *Fusarium moniliforme*, and *Rhizoctonia solani*. Two types of ZnNPs were compared: those synthesized by selected endophytic fungal isolates (EF-ZnNPs) and those derived from olive mill waste (OMW-ZnNPs). Each type was tested at three concentrations (50, 100, and 150 ppm) under in vitro conditions.

3.8.1. Radial growth inhibition (%) of pathogenic fungi by ZnNPs

The results showed a concentration-dependent increase in antifungal activity for both nanoparticle sources. However, EF-ZnNPs consistently demonstrated higher inhibition percentages across all pathogens and concentrations compared to OMW-ZnNPs (Table 6). *Fusarium oxysporum* exhibited the highest sensitivity to EF-ZnNPs, with inhibition rates reaching 72.7% at 150 ppm,

followed by *F. moniliforme* (69.1%) and *R. solani* (66.9%). In contrast, the maximum inhibition recorded for OMW-ZnNPs at 150 ppm was lower, ranging from 58.6% to 63.6% depending on the pathogen. The enhanced efficacy of EF-ZnNPs may be attributed to the uniform morphology, smaller particle size, and biologically active surface coatings imparted during fungal-mediated synthesis. Such nanoparticles are likely to disrupt fungal cell walls more efficiently and interfere with metabolic processes. These findings align with previous studies reporting the superior antifungal properties of mycosynthesized ZnNPs over chemically or agro-waste derived counterparts due to their reactive surface properties and higher bioavailability (Raliya *et al*., 2013; Navin *et al*., 2018). The statistical analysis using Duncan's multiple range test confirmed significant differences ($p < 0.05$) between treatments, and the letters assigned next to the values in Table 6 represent homogeneous groups. Accordingly, EF-ZnNPs were selected as the more promising candidate for subsequent in vivo evaluation, based on their superior performance in inhibiting the most aggressive fungal pathogens affecting potato crops. The endophytic fungi-derived ZnNPs demonstrated superior antifungal efficiency, particularly at higher concentrations, making them more suitable for integrated disease management strategies in potato cultivation. Based on these findings, EF-ZnNPs will be prioritized in the next stage of the study, including greenhouse evaluation and formulation trials.

Table 6: Radial growth inhibition (%) of pathogenic fungi by ZnNPs synthesized using endophytes (EF-ZnNPs) and olive mill waste (OMW-ZnNPs) at different concentrations

Pathogen	ZnNP Source	50 ppm	100 ppm	150 ppm
Fusarium oxysporum	EF-ZnNPs	49.7 ± 1.4 b	63.0 ± 1.3 a	72.7 ± 1.1 a
	OMW-ZnNPs	41.6 ± 1.2 c	54.1 ± 1.6 b	62.1 ± 1.3 b
Fusarium moniliforme	EF-ZnNPs	46.3 ± 1.5 b	59.9 ± 1.2 a	69.1 ± 1.4 a
	OMW-ZnNPs	37.8 ± 1.3 c	51.2 ± 1.5 b	58.7 ± 1.2 b
Rhizoctonia solani	EF-ZnNPs	44.0 ± 1.3 b	57.7 ± 1.1 a	66.9 ± 1.2 a
	OMW-ZnNPs	35.7 ± 1.1 c	48.4 ± 1.4 b	57.1 ± 1.3 b

Mean ± SE; values with different letters in the same row differ significantly according to Duncan's test, $p < 0.05$.

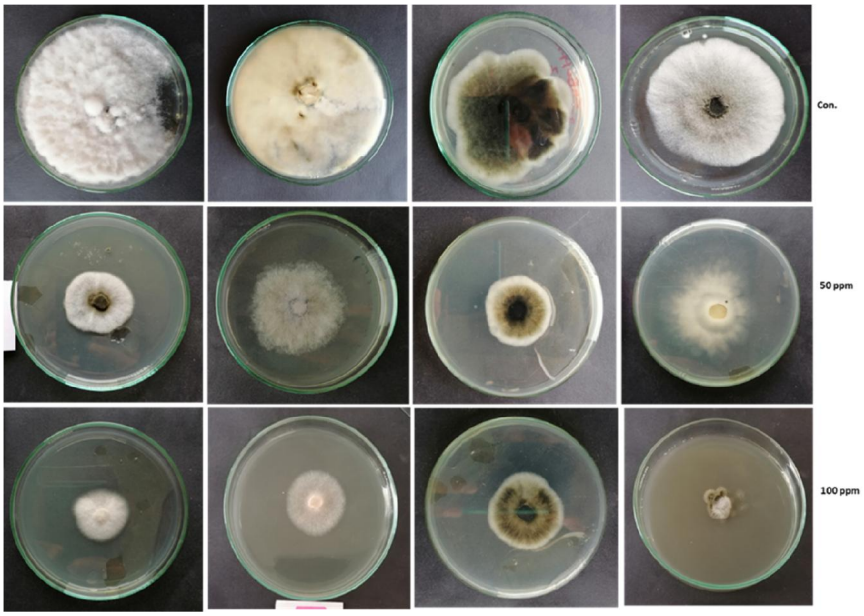

Fig. 4: Petri plate images show the inhibition of *Fusarium* spp. by ZnNPs synthesized using endophytic fungi at 50 and 100 ppm. A clear reduction in fungal growth is observed compared to controls, confirming the antifungal potential of the biosynthesized nanoparticles.

3.8.2 Dry mycelial weight assay

To further assess the antifungal efficacy of biosynthesized ZnNPs, treated fungal isolates were cultivated in liquid potato dextrose broth supplemented with ZnNPs at three concentrations (50, 100, and 150 ppm). Both nanoparticle types those synthesized by endophytic fungi and those derived from olive mill waste (OMW) were tested. After seven days of incubation under static conditions, the fungal mycelia were harvested, dried, and weighed. The results showed a clear concentration-dependent reduction in mycelial biomass across all tested pathogens. ZnNPs synthesized by endophytic fungi (especially from *Trichoderma* sp.) significantly outperformed the OMW-derived ZnNPs in suppressing fungal growth. At 150 ppm, *Fusarium oxysporum, Rhizoctonia solani*, and *Pythium ultimum* exhibited the most pronounced reductions in dry weight (ranging from 63 % to 70.3%) with fungal-derived ZnNPs, compared to 55.8–60.3% reduction using OMW-derived nanoparticles.

These differences were statistically significant ($p \leq 0.05$), as confirmed by Duncan's multiple range test (Table 7), suggesting that the origin and synthesis pathway of ZnNPs influence their bioavailability and interaction with fungal cell membranes.

Table 7: Dry mycelial weight reduction (%) of three pathogenic fungi treated with endophytic- and OMW-derived ZnNPs at three concentrations (mean ± se)

Pathogen	*ZnNP Source*	50 ppm	100 ppm	150 ppm
Fusarium oxysporum	EF-ZnNPs	47.1 ± 1.4 d	60.3 ± 1.2 c	72.7 ± 1.1 a
	OMW-ZnNPs	43.4 ± 1.7 e	56.0 ± 1.3 d	67.9 ± 1.0 b
Fusarium moniliforme	EF-ZnNPs	44.7 ± 1.3 d	58.5 ± 1.5 c	70.2 ± 1.3 a
	OMW-ZnNPs	40.0 ± 1.6 e	53.1 ± 1.4 d	65.1 ± 1.2 b
Rhizoctonia solani	EF-ZnNPs	42.3 ± 1.5 d	57.4 ± 1.4 c	69.3 ± 1.2 a
	OMW-ZnNPs	38.6 ± 1.3 e	51.6 ± 1.2 d	63.5 ± 1.0 b

3.8.3 Spore Morphology Observation

Microscopic examination of fungal spores exposed to ZnNPs (150 ppm) was conducted to evaluate sub-lethal structural alterations. Spores from cultures treated with fungal derived ZnNPs showed marked abnormalities including collapsed walls, irregular shapes, and disrupted septa especially in *Fusarium oxysporum*. In contrast, spores treated with OMW-derived ZnNPs retained relatively intact morphology with less frequent deformities. These structural disruptions are consistent with the mode of action of metallic nanoparticles, which are believed to induce oxidative stress, membrane destabilization, and interference with cytoplasmic content (Iravani, 2011). The more intense alterations observed with fungal-based ZnNPs suggest enhanced nanoparticle–pathogen interaction, possibly due to smaller particle size or higher surface reactivity.

Overall, these findings reinforce the superior antifungal potential of ZnNPs synthesized by endophytic fungi and justify their selection for subsequent in vivo applications.

3.9. Greenhouse Evaluation of ZnNPs Efficacy and Their Impact on Soil Fungal Load

To assess the *in vivo* performance of biosynthesized zinc nanoparticles (ZnNPs), greenhouse trials were conducted during 2022/2023 winter season using the most effective concentrations identified from in vitro experiments (100 and 150 ppm). The evaluation focused on two key aspects: the ability of ZnNPs to suppress disease symptoms and improve plant health, and their broader effect on fungal populations in the rhizosphere.

3.9.1 Disease Suppression and Growth Performance

Treated potato plants grown in pathogen-infested soil showed a significant reduction in disease incidence and severity compared to untreated controls. EF-ZnNPs (derived from endophytic fungi) demonstrated superior protective effects, reducing disease severity indices (DSI) of *Fusarium*

oxysporum, *F. moniliforme*, and *Rhizoctonia solani* by 55–68%. In contrast, plants treated with OMW-ZnNPs showed a 42–58% reduction in DSI (Table 8).

Notably, EF-ZnNPs treatments also improved plant growth parameters, including shoot length, root biomass, and overall vigor. These improvements may be attributed to the dual action of ZnNPs: direct antifungal activity and indirect stimulation of plant defence

3.9.2 Rhizosphere Fungal Population Dynamics

Analysis of soil samples revealed a marked decrease in total fungal count (CFU/g soil) in ZnNP-treated pots. The rhizosphere fungal load decreased by 40–55% under EF-ZnNPs, and by 30–45% under OMW-ZnNPs, compared to the pathogen-only control (Table 8). This suggests that ZnNPs not only target specific phytopathogens but also exert a broader antifungal effect in the rhizosphere. However, the reduction in total fungal load was more controlled in EF-ZnNP treatments, possibly due to more selective targeting of harmful species while sparing beneficial microbial populations.

Table 8: Effect of EF-ZnNPs and OMW-ZnNPs on Disease Severity Index (DSI%) and Rhizosphere Fungal Load greenhouse

Pathogen	ZnNPs Treatment	DSI (%)	Fungal Load (CFU ×10³/g)
Fusarium oxysporum	EF-ZnNPs (100)	39.8 ± 1.3 c	13.4 ± 0.5 c
	EF-ZnNPs (150)	30.2 ± 1.2 d	10.6 ± 0.4 d
	OMW-ZnNPs (100)	49.1 ± 1.4 b	16.6 ± 0.5 b
	OMW-ZnNPs (150)	39.1 ± 1.2 c	13.8 ± 0.6 c
	Control	71.8 ± 1.6 a	25.0 ± 0.7 a
F. moniliforme	EF-ZnNPs (100)	38.4 ± 1.2 c	13.1 ± 0.4 c
	EF-ZnNPs (150)	27.0 ± 1.1 d	11.3 ± 0.5 d
	OMW-ZnNPs (100)	46.9 ± 1.3 b	15.3 ± 0.6 b
	OMW-ZnNPs (150)	36.2 ± 1.3 c	14.6 ± 0.5 c
	Control	64.9 ± 1.5 a	23.5 ± 0.8 a
Rhizoctonia solani	EF-ZnNPs (100)	36.2 ± 1.2 c	14.5 ± 0.4 c
	EF-ZnNPs (150)	24.5 ± 1.1 d	12.4 ± 0.3 d
	OMW-ZnNPs (100)	44.8 ± 1.3 b	17.3 ± 0.6 b
	OMW-ZnNPs (150)	34.4 ± 1.2 c	15.5 ± 0.5 c
	Control	61.7 ± 1.4 a	25.3 ± 0.7 a
Pathogen Mix (All)	EF-ZnNPs (100)	42.2 ± 1.3 c	15.7 ± 0.5 c
	EF-ZnNPs (150)	32.4 ± 1.2 d	12.5 ± 0.4 d
	OMW-ZnNPs (100)	52.3 ± 1.5 b	19.0 ± 0.5 b
	OMW-ZnNPs (150)	40.2 ± 1.3 c	16.3 ± 0.5 c
	Control	74.2 ± 1.6 a	28.4 ± 0.6 a

Values with different letters in the same row differ significantly at $p < 0.05$ according to Duncan's test.

4. Conclusion

This study demonstrated the dual biotechnological potential of endophytic fungi isolated from healthy potato plants cultivated under arid conditions in Egypt. The isolates not only exhibited selective antagonistic activity against major soil-borne pathogens such as *Fusarium oxysporum*, *F. moniliforme*, and *Rhizoctonia solani*, but also successfully mediated the biosynthesis of Zinc nanoparticles (ZnNPs) with significant antifungal efficacy. Among the tested genera, *Trichoderma* sp. and *Penicillium* sp. showed the most consistent biocontrol performance *in vitro*, while isolates of *Fusarium spp.* and *Aspergillus sp.* proved highly effective in ZnNPs biosynthesis, with UV–Vis absorption peaks ranging between 365–390 nm. Comparatively, ZnNPs synthesized by endophytes (EF-ZnNPs) outperformed those synthesized from olive mill waste (OMW-ZnNPs) in suppressing pathogen growth and reducing disease severity under greenhouse conditions. EF-ZnNPs not only decreased the disease severity index (DSI) significantly but also led to a more controlled reduction in rhizosphere fungal load, indicating a promising selective antifungal action. Moreover, the 150 ppm concentration of EF-ZnNPs emerged as the most effective treatment, enhancing plant growth and limiting fungal spread more efficiently than OMW-ZnNPs at the same dose. The findings emphasize the integrated potential of endophytic fungi both as biocontrol agents and nanomaterial biofactories, offering a sustainable and eco-friendly strategy for managing potato root diseases. However, while the results are promising, further investigations are warranted to assess the biosafety and environmental impact of the synthesized ZnNPs under field conditions, particularly their long-term effects on soil microbiota, plant health, and food safety.

References

Alkhalaf , M.I., M.R.H. Hussein, and M. Hamza, 2020. Green synthesis of silver nanoparticles by Nigella sativa extract alleviates diabetic neuropathy through anti-inflammatory and antioxidant effects. Saudi Journal of Biological Sciences 27: 2410–2419.

Atlas, R.M. and L.C. Parks, 1997. Handbook of Microbiological Media, 2nd ed. Boca Raton: CRC Press.

Attia, Attia, M.F.; Abada, K.A.; Naffa, A.M.A.K and Boghdady, S.F. 2019. Management of potato post-harvest dry rot by organic acids and oils. Egyptian Journal of Phytopathology, 47(1): 261–270.

Aydi-Ben-Abdallah, R., Jabnoun-Khiareddine H. and Daami-Remadi M. (2020). Fusarium wilt biocontrol and tomato growth stimulation, using endophytic bacteria naturally associated with Solanum sodomaeum and S. bonariense plants.

Azil, N., Stefańczyk, E., Sobkowiak, S. et al. 2021. Identification and pathogenicity of Fusarium spp. associated with tuber dry rot and wilt of potato in Algeria. Eur J Plant Pathol 159, 495–509. https://doi.org/10.1007/s10658-020-02177-5

Barnett, H.L. and B.B. Hunter, 1972. Illustrated Genera of Imperfect Fungi, 3rd ed. Minneapolis: Burgess Publishing Company.

Bell, D.K., H.D. Wells, and C.R. Markham, 1982. *In vitro* antagonism of Trichoderma spp. against six fungal plant pathogens. Phytopathology, 72(4): 379–382.

Burlakoti, R. R., and Sapkota, S. 2020. Root rot and wilting disease complex of red raspberry in the Fraser Valley of British Columbia in 2018 and 2019. Canadian Plant Disease Survey,100: Disease highlights. Can. J. Plant Pathol. 42. https://doi.org/10.1080/07060661.2020.1752524

De Matteis, V., L. Rizzello, and R. Rinaldi, 2021. Purification of olive mill wastewater through noble metal nanoparticle synthesis: waste safe disposal and nanomaterial impact on healthy hepatic cell mitochondria. Environmental Science and Pollution Research, 28: 26154–26171.

Dennis, C. and J. Webster, 1971. Antagonistic properties of species-groups of Trichoderma. I. Production of non-volatile antibiotics. Transactions of the British Mycological Society, 57(1): 25–39.

Domsch, K.H., W. Gams, and T.H. Anderson, 2007. Compendium of Soil Fungi, 2nd edn. Eching: IHW-Verlag.

Elsayed, N., M. S. Hasanin, M. Abdelraof, 2022. Utilization of olive leaves extract coating incorporated with zinc/selenium oxide nanocomposite to improve the postharvest quality of green beans pods, Bioactive Carbohydrates and Dietary Fibre, Volume 28, 100333.

Fadiji, Ayomide Emmanuel, Peter Edward Mortimer, Jianchu Xu, Eno E. Ebenso, and Olubukola Oluranti Babalola. 2022. "Biosynthesis of Nanoparticles Using Endophytes: A Novel Approach for Enhancing Plant Growth and Sustainable Agriculture" Sustainability 14, no. 17: 10839. https://doi.org/10.3390/su141710839

Hafeez, B., Y. M. Khanif, and M. Saleem. 2013. Role of Zinc in Plant Nutrition- A Review. Journal of Experimental Agriculture International 3 (2):374-91. https://doi.org/10.9734/AJEA/2013/2746

Harman, G.E., C.R. Howell, A. Viterbo, I. Chet, and M. Lorito, 2004. Trichoderma species opportunistic, avirulent plant symbionts. Nature Reviews Microbiology, 2(1): 43–56

Hasansab A. Nadaf, G.V. Vishaka, M. Chandrashekharaiah, M.S. Rathore, C. Srinivas, Ravi V. Mural, 2022. Biological synthesis of metal nanoparticles by microorganisms: a sustainable approach, Microbial Resource Technologies for Sustainable Development, Elsevier:269-288. https://doi.org/10.1016/B978-0-323-90590-9.00021-3.

He, L., Y. Liu, A. Mustapha, and M. Lin, 2020. Antifungal activity of zinc oxide nanoparticles against *Botrytis cinerea* and *Penicillium expansum*. Microbiological Research, 240: 126538.

Iravani, S., 2011. Green synthesis of metal nanoparticles using plants. Green Chemistry, 13(10): 2638–2650.

Iravani, S., R.S. Varma, and S. Rastooghi, 2023. Plant-based synthesis of metal nanoparticles: Recent advances and future prospects. Green Chemistry Letters and Reviews, 16(1): 1-24.

Jain, N., A. Bhargava, J.C. Tarafdar, S.K. Singh, and J. Panwar, 2012. A biomimetic approach towards synthesis of zinc oxide nanoparticles. Applied Microbial Biotechnol., 012:3934-2.

Leslie, J.F. and B.A. Summerell, 2006. The Fusarium Laboratory Manual. Ames: Blackwell Publishing.

McGovern, R.J., 2015. Management of tomato diseases caused by *Fusarium oxysporum*. Crop Protection, 73: 78–92.

McKinney, H.H., 1923. A new system of grading plant diseases. Journal of Agricultural Research, 26(2): 195–218.

Mosquera-Sánchez, L.P., P.A. Arciniegas-Grijalba, M.C. Patiño-Portela, B.E. Guerra–Sierra, J.E. Muñoz-Florez, J.E. Rodríguez-Páez, 2020. Antifungal effect of zinc oxide nanoparticles (ZnO-NPs) on Colletotrichum sp., causal agent of anthracnose in coffee crops, Biocatalysis and Agricultural Biotechnology, 25, 101579, https://doi.org/10.1016/j.bcab.2020.101579.

Mukherjee, P.K., B.A. Horwitz, A. Herrera-Estrella, M. Schmoll, and C.M. Kenerley, 2020. Trichoderma research in the genome era. Annual Review of Phytopathology, 58: 447–465.

Navin Kumar, Debjyoti Banerjee, Reynaldo Chavez, 2018. Exploring additives for improving the reliability of zinc nitrate hexahydrate as a phase change material (PCM), Journal of Energy Storage, 20: 153-162, https://doi.org/10.1016/j.est.2018.09.005.

Nelson, P.E., T.A. Toussoun, and W.F.O. Marasas, 1983. Fusarium Species: An Illustrated Manual for Identification. University Park: Pennsylvania State University Press.

Ondřej M., R. Dostálová and R. Trojan, 2008. Evaluation of virulence of *Fusarium solani* isolates on pea. Plant Protect. Sci.,44: 9–18.

Rajani, Preeti Mishra, Sarita Kumari, Parmila Saini, Rishi Kesh Meena, Role of nanotechnology in management of plant viral diseases, Materials Today: Proceedings, 69, 1:1-10

Raliya, R., J.C. Tarafdar, P. Biswas, and V. Saharan, 2013. ZnO nanoparticles induced synthesis of polysaccharides and phosphatases in clusterbean (*Cyamopsis tetragonoloba* L.). Agricultural Research, 2(1): 48–57.

Russo, E., A. Spallarossa, A. Comite, M. Pagliero, P. Guida, V. Belotti, D. Caviglia and A.M. Schito, 2022. Valorization and Potential Antimicrobial Use of Olive Mill Wastewater (OMW) from Italian Olive Oil Production. Antioxidants (Basel). 4;11(5):903. doi: 10.3390/antiox11050903. PMID: 35624767; PMCID: PMC9137489.

Saber, M.M. et al., 2013. Biochemical changes of potato cultivars due to infection by dry rot disease (*Fusarium* spp.) in Egypt. Egyptian Journal of Phytopathology, 41(1): 53–65.

Schulz, B. and C. Boyle, 2005. The endophytic continuum. Mycological Research, 109(6): 661–686.

Singh, P., Y.J. Kim, D. Zhang, and D.C. Yang, 2016. Biological synthesis of nanoparticles from plants and microorganisms. Trends in Biotechnology, 34(7): 588–599.

Strobel, G. and B. Daisy, 2003. Bioprospecting for microbial endophytes and their natural products. Microbiology and Molecular Biology Reviews, 67(4): 491–502.

Techaoei, S., C. Jirayuthcharoenkul, K. Jarmkom, T. Dumrongphuttidecha and W. Khobjai, 2020. Chemical evaluation and antibacterial activity of novel bioactive compounds from endophytic fungi in Nelumbo nucifera. Saudi J Biol Sci., 27(11):2883-2889.

Vincent, J.M., 1947. Distortion of fungal hyphae in the presence of certain inhibitors. Nature, 159(4051): 850.

Zachary A. Noel, L.V. Roze, M. Breunig, and F. Trail 2022. Endophytic Fungi as a Promising Biocontrol Agent to Protect Wheat from *Fusarium graminearum* Head Blight. Endophytic Fungi as a Promising Biocontrol Agent to Protect Wheat from *Fusarium graminearum* Head Blight.